Error analysis and optimal design of polarization calibration unit for solar telescope*

Jun-Feng Hou(侯俊峰)†, Dong-Guang Wang(王东光), Yuan-Yong Deng(邓元勇), Ying-Zi Sun(孙英姿), and Zhi-Yong Zhang(张志勇)

Key Laboratory of Solar Activity, National Astronomical Observatories, Chinese Academy of Sciences, Beijing 100012, *China*

(Received 13 March 2017; revised manuscript received 4 April 2017; published online 10 July 2017)

Polarization calibration unit (PCU) has become an indispensable element for solar telescopes to remove the instrumental polarization; the polarimetric accuracy of calibration depends strongly on the properties of PCU. In the paper, we analyze the measurement errors induced by PCU based on polarized light theory and find that the imperfections of the waveplate generate the main calibration errors. An optimized calibration method is proposed to avoid the effects from waveplate imperfections, and a numerical simulation is given to evaluate the polarization accuracy by analyzing the relation between calibration error and intensity instability. The work is very important for solar telescopes with high polarization precision up to 10^{-4} I_c.

Keywords: solar telescope, polarization calibration

PACS: 95.55.Cs, 95.55.Ev, 95.75.Hi **DOI:** 10.1088/1674-1056/26/8/089501

1. Introduction

Magnetic field is one of the most important physical quantities in the study of solar physics. All the phenomena and processes in the sun are closely related to the solar magnetic field. At present, the solar magnetic field is mainly measured by polarization technique based on Zeeman effect theory and the polarized radiation transfer model of the solar atmosphere,[1,2] especially in the visible and near infrared wavelength region. Therefore, polarization measurement[3,4] is the core technology of the solar telescope. Now the next-generation large-aperture solar telescopes are expected to achieve extremely high polarization measurement accuracy. For example, the 4-meter Daniel K. Inouye Solar Telescope (DKIST)[5] in USA and European Solar Telescope (EST)[6] are required to reach up to 5×10^{-4} I_c (I_c is the continuum intensity of standard solar spectrum). Moreover, the 8-meter China Giant Solar Telescope (CGST)[7] proposed by China is required even to reach up to 2×10^{-4} I_c. How to realize the high-accuracy polarization measurement becomes the most important technical index for large-aperture solar telescopes to obtain the accurate magnetic field observation.

Most large-aperture solar telescopes usually employ a Gregorian main optical system and an Alt–Azimuth tracking mount to guide solar image into the Coude room. For the Gregorian main optical system, geometrical optics includesonly primary and secondary mirrors, it will have a very small instrumental polarization and can be neglected for solar polarization signals at 10^{-4} I_c level if the optical system is symmetric. Conversely, if the optical system is off-axis, then it will have a little large instrumental polarization. However, the instrumental polarization is fixed and can be calibrated accurately by some methods,[8–10] which is beyond the scope of our paper. In comparison, the instrumental polarization mainly comes from the Alt–Azimuth mounted optics between Gregorian focus and Stokes polarimeter, and it gives rise to large crosstalk among Stokes parameters *IQUV* and also varies strongly with time.[11] Therefore, the classical calibration strategy for solar telescopes is to place a group of polarization calibration units (PCUs) near Gregorian focus of telescope to calibrate the instrumental polarization of the whole Alt–Azimuth mounted optics between Gregorian focus and Stokes polarimeter.[12] In this case, polarization accuracy depends on the properties of PCU, which is usually taken as an ideal and standard Stokes generator to obtain the pure linear polarization and circular polarization.[13,14] However, it is important to understand that nothing is perfect. Some effects of a non-ideal PCU, such as polarization parameter variation with spectrum and space due to manufacture error, interference, the misalignment of optic axis and calibration optics design, etc., will affect the polarization calibration and lead to a loss of polarization accuracy.

In this paper, we analyze the main measurement errors induced by PCU and optimize its calibration method to improve calibration accuracy up to 10^{-4} I_c.

The rest of this paper is organized as follows. In Section 2 the PCU and calibration method are described. In Section 3 the error analysis of an imperfect PCU is made. In Section 4, an improved polarization calibration method is designed; a numerical simulation error analysis is given and discussed. Finally, some conclusions are drawn from this study in Section 5.

*Project supported by the National Natural Science Foundation of China (Grant Nos. 11403047, 11427901, 11178005, 11373044, 11273034, and 11373042).

†Corresponding author. E-mail: jfhou@bao.ac.cn

© 2017 Chinese Physical Society and IOP Publishing Ltd

2. Polarization calibration unit (PCU) and calibration process

Figure 1 shows the schematic diagram for polarization calibration of solar telescope. There are two identical PCUs, one is placed near Gregorian focus plane to calibrate the instrumental polarization of Alt–Azimuth mounted optics, and the other is placed behind the Coude focus to calibrate the Stokes polarimeter. The PCU consists of a polarizer and a quarter waveplate, a group of known incident Stokes vectors can be obtained by rotating both elements from 0° to 360° separately.

According to polarized light and Mueller matrix theory, assume that $\boldsymbol{X}$ is the polarized response matrix of Stokes polarimeter, $\boldsymbol{M}_{\mathrm{T}}$ is the mueller matrix representing the instrumental polarization of Alt–Azimuth mounted optics, and $\boldsymbol{X}'$ is the polarized response matrix of the whole telescope combined with Alt–Azimuth mounted optics and Stokes polarimeter. Theoretically,

$$\boldsymbol{X}' = \boldsymbol{X} \times M_{\mathrm{T}}. \tag{1}$$

In a real polarization calibration process, all the optical system behind PCU, including Alt–Azimuth mounted optics and polarimeter, can be seen as a blackbody under calibration according to the following steps:

Step 1 insert the second PCU into the optical path to calibrate the Stokes polarimeter, and obtain the response matrix $\boldsymbol{X}$;

Step 2 move the second PCU out and insert the first PCU into the optical path to calibrate the whole telescope, and obtain the response matrix $\boldsymbol{X}'$;

Step 3 calculate instrumental polarization $\boldsymbol{M}_{\mathrm{T}}$ of the Alt–Azimuth mounted optics by $\boldsymbol{X}^{-1} \times \boldsymbol{X}'$.

Obviously, polarization calibration accuracy depends strongly on properties of PCUs. The Stokes polarimeter is a little easy to calibrate to a very high accuracy[15,16] even if the second PCU is not perfect because they are placed in Coude room and the properties are stable, but not for Alt–Azimuth mounted optics nor the first PCU. Therefore, it is necessary and important for solar telescope to be used to analyze and optimize the first PCU and its calibration method.

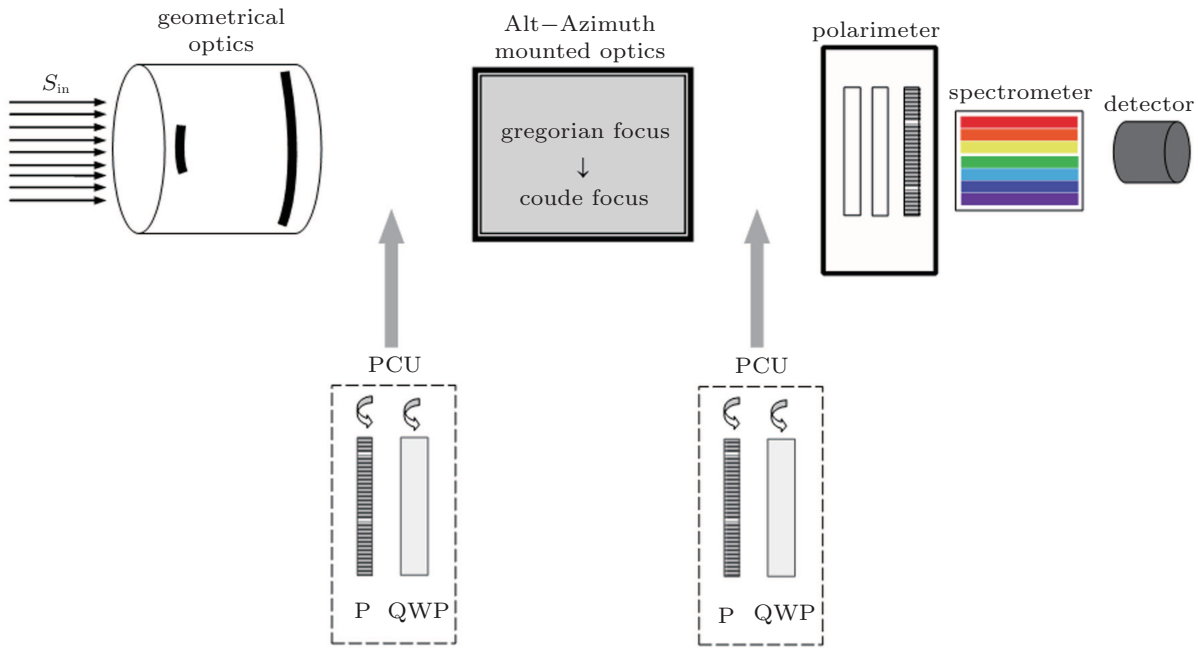


Fig. 1. (color online) Schematic diagram for polarization calibration of solar telescope.

3. Error analysis of an imperfect PCU

3.1. Polarization calibration requirement

Polarization calibration requirement can be best described by the tolerance matrix Δ as Eq. (2) defined by Ichimoto *et al.* at 2008,[16] where ε is polarization accuracy of a telescope, q, u, and v are the max linear polarization and circular polarization at sunspot respectively. The real tolerance requirement will be calculated by Eq. (2) if we assume $q = u = v = 0.1\ I_{\mathrm{c}}$ and $\varepsilon = 10^{-4}\ I_{\mathrm{c}}$ as shown in Eq. (3), which indicates that the crosstalk is 10^{-4} from I to Q, U, V, and 10^{-3} among Q, U, and V for Stokes vector. It is noted that the crosstalk 10^{-4} from I to Q, U, and V can regularly calibrated by solar continuum polarization measurement, what we concern in the paper is to analyze an imperfect PCU and to see how to reduce PCU's crosstalk among I, Q, U, and V to 10^{-3}.

$$\Delta = \begin{bmatrix} \varepsilon & \varepsilon/q & \varepsilon/u & \varepsilon/v \\ \varepsilon & \varepsilon/q & \varepsilon/u & \varepsilon/v \\ \varepsilon & \varepsilon/q & \varepsilon/u & \varepsilon/v \\ \varepsilon & \varepsilon/q & \varepsilon/u & \varepsilon/v \end{bmatrix}, \tag{2}$$

$$\Delta_{10^{-4}I_c} = \begin{bmatrix} - & 10^{-3} & 10^{-3} & 10^{-3} \\ 10^{-4} & 10^{-3} & 10^{-3} & 10^{-3} \\ 10^{-4} & 10^{-3} & 10^{-3} & 10^{-3} \\ 10^{-4} & 10^{-3} & 10^{-3} & 10^{-3} \end{bmatrix}. \quad (3)$$

3.2. Error analysis of an imperfect PCU

The error analysis is made for an imperfect PCU in this subsection to see what factors are the main error sources, which limit the polarization calibration accuracy of PCU up to 10^{-4} I_c. Four error sources, including the manufacture error, interference, misalignment of fast axis and Field of view effect, are analyzed.

According to the theory of polarized light, the incident light from the Sun is conventionally described through the Stokes vector $\boldsymbol{S}_{\text{in}} = [I\ Q\ U\ V]^{\text{T}}$, where I is the intensity, Q and U are two independent linear polarizations, and V is the circular polarization. The polarization properties of any polarized element before and after the light beam has passed through, can be conveniently described by a 4×4 Mueller matrix $\boldsymbol{M}$. In other words, Mueller matrix $\boldsymbol{M}$ is the eigenmatrix of the polarized element and represents the relation between the incident Stokes vector $\boldsymbol{S}_{\text{in}}$ and the exit Stokes vector $\boldsymbol{S}_{\text{out}}$, expressed by the formula $\boldsymbol{S}_{\text{out}} = \boldsymbol{M} \times S_{\text{in}}$. In the following, all the error analysis focuses on the Mueller matrix of each polarized element in PCU, by calculating the tolerance of each of error sources to make sure that the crosstalk among $I\ Q\ U\ V$ is below 10^{-3} (equivalently, to ensure that the absolute error of each element in Mueller matrix is below 10^{-3}).

3.2.1. Manufacture error

The manufacture error is inevitable for any polarized element in PCU, which may lead to the low extinction ratio of polarizer and the large retardation error and nonuniformity of quarter waveplate.

$$\boldsymbol{M}_{\text{p}} = \begin{bmatrix} 1 & \dfrac{ER-1}{ER+1} & 0 & 0 \\ \dfrac{ER-1}{ER+1} & 1 & 0 & 0 \\ 0 & 0 & \dfrac{2\sqrt{ER}}{ER+1} & 0 \\ 0 & 0 & 0 & \dfrac{2\sqrt{ER}}{ER+1} \end{bmatrix}, \quad (4)$$

$$\boldsymbol{M}_{\text{p}}^{ER\to\infty} = \begin{bmatrix} 1 & 1 & 0 & 0 \\ 1 & 1 & 0 & 0 \\ 0 & 0 & 0 & 0 \\ 0 & 0 & 0 & 0 \end{bmatrix}. \quad (5)$$

Generally, a polarizer's eigen Mueller matrix can be described by Eq. (4), where ER is the extinction ratio. When ER tends to infinity (∞) the polarizer acts as an ideal polarizer and its eigen Mueller matrix is written as Eq. (5). Practically, ER is not infinity due to manufacture limit, it mainly reduces the polarization degree of incident light and induces crosstalk between Stokes U and V. Mueller matrix error $\Delta\boldsymbol{M}_{\text{p}}$ of a polarizer can be calculated from $\Delta\boldsymbol{M}_{\text{p}} = |\boldsymbol{M}_{\text{p}} - \boldsymbol{M}_{\text{p}}^{ER\to\infty}|$, where only $\Delta\boldsymbol{M}_{\text{p}}(1,2)$, $\Delta\boldsymbol{M}_{\text{p}}(2,1)$, $\Delta\boldsymbol{M}_{\text{p}}(3,3)$, and $\Delta\boldsymbol{M}_{\text{p}}(4,4)$ are not zero, moreover, $\Delta\boldsymbol{M}_{\text{p}}(1,2) = \Delta\boldsymbol{M}_{\text{p}}(2,1)$, and $\Delta\boldsymbol{M}_{\text{p}}(3,3) = \Delta\boldsymbol{M}_{\text{p}}(4,4)$. Figure 2 shows the relationship between $\boldsymbol{M}_{\text{p}}(1,2)$ and $\boldsymbol{M}_{\text{p}}(3,3)$ and the extinction ratio ER. Obviously, the maximal error is from $\boldsymbol{M}_{\text{p}}(3,3)$ and $\boldsymbol{M}_{\text{p}}(4,4)$, but their values can be relaxed to 0.1 because the normalized Stokes vector from sun incident into the polarizer is less than 0.01 in magnitude. By comparison, $\boldsymbol{M}_{\text{p}}(1,2)$ and $\boldsymbol{M}_{\text{p}}(2,1)$ are required to reach 10^{-3} and the extinction ratio ER must be larger than 2000:1.

$$\boldsymbol{M}_{\text{wp}} = \begin{bmatrix} 1 & 0 & 0 & 0 \\ 0 & 1 & 0 & 0 \\ 0 & 0 & \cos\delta & \sin\delta \\ 0 & 0 & -\sin\delta & \cos\delta \end{bmatrix}, \quad (6)$$

$$\boldsymbol{M}_{QWP} = \begin{bmatrix} 1 & 0 & 0 & 0 \\ 0 & 1 & 0 & 0 \\ 0 & 0 & 0 & 1 \\ 0 & 0 & -1 & 0 \end{bmatrix}. \quad (7)$$

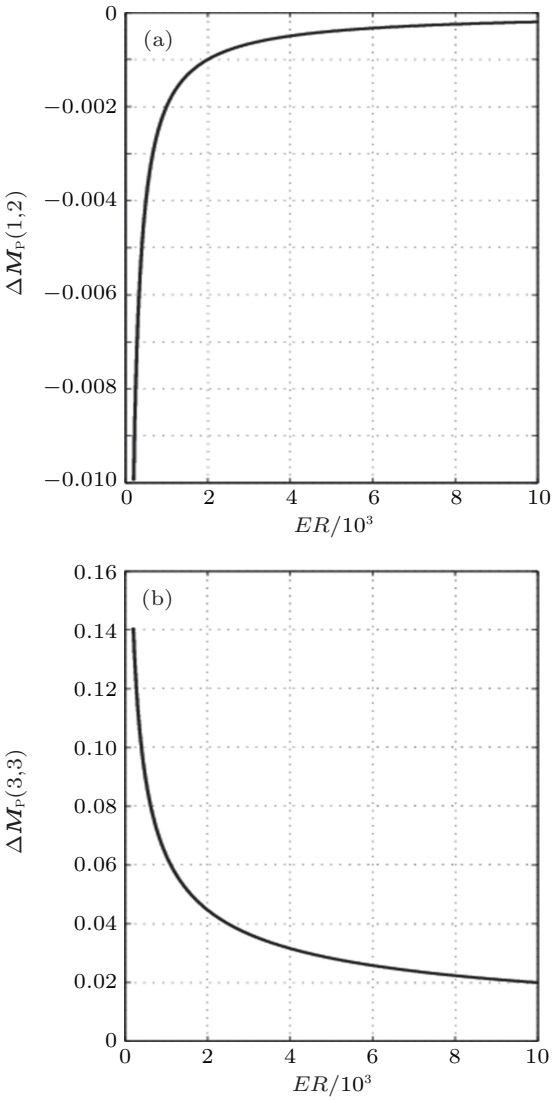


Fig. 2. Dependence of Mueller matrix element errors (a) $\Delta\boldsymbol{M}_{\text{p}}(1,2)$ and (b) $\Delta\boldsymbol{M}_{\text{p}}(3,3)$ of a polarizer on extinction ratio ER.

A pure waveplate's eigen Mueller matrix can be described by Eq. (6), where δ is the retardation. When $\delta = \pi/2$, its Mueller matrix is written as Eq. (7). Retardation error comes from the thickness error of a waveplate in manufacture, and it leads to the retardation of quarter waveplate deviating from the $\pi/2$, and will induce the crosstalk between linear polarization and circular polarization. Mueller matrix error $\Delta M_{\rm wp}$ of quarter waveplate can be calculated from $\Delta M_{\rm wp} = |M_{\rm wp} - M_{\rm QWP}|$, where only $\Delta M_{\rm wp}(3,3)$, $\Delta M_{\rm wp}(3,4)$, $\Delta M_{\rm wp(4,3)}$, and $\Delta M_{\rm wp}(4,4)$ are not zero, and also, $\Delta M_{\rm wp}(3,3) = \Delta M_{\rm wp}(4,4)$, and $\Delta M_{\rm wp}(3,4) = \Delta M_{\rm wp}(4,3)$. Figure 3 exhibits the relationship between $\Delta M_{\rm wp}(3,3)$ and $\Delta M_{\rm wp}(3,4)$ and retardation error $\Delta\delta = \delta - \pi/2$, and it is required that retardation error is less than 0.001 rad if crosstalk is less than 10^{-3} among I, Q, U, and V.

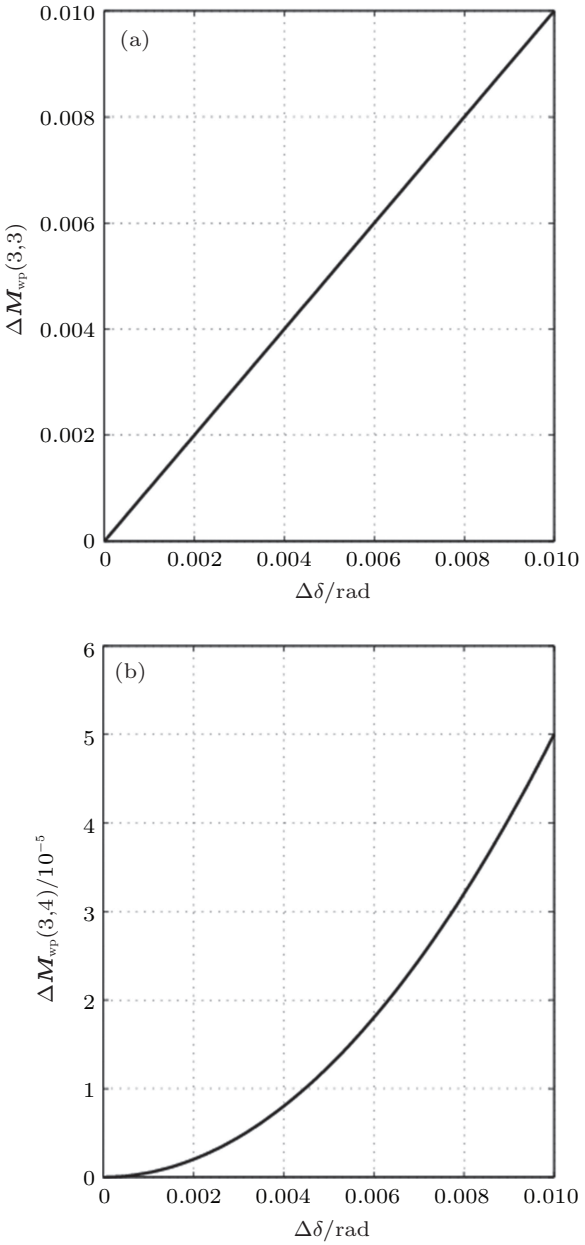


Fig. 3. Dependence of Mueller matrix element errors (a) $\Delta M_{\rm wp}(3,3)$ and (b) $\Delta M_{\rm wp}(3,4)$ of a quarter waveplate on retardation error $\Delta\delta$.

3.2.2. Interference

Multiple-beam interference behaves identically to a Fabry–Pérot interferometer. As a consequence of the fundamental nature of the device, any waveplate also acts as a weak partial polarizer. The weak polarization arises from the difference between the reflectance of the waveplate face for fast and that for slow axis.[17] Effects from this property affect dichroism in wavelength, especially, the transmittances of fast and slow axis are not the same and oscillate with wavelength. The effect cannot be completely eliminated even if it can be degraded by an anti-reflective coating. The waveplate's eigen Mueller matrix with interference can be described by Eqs. (8) and (9), where R is the reflectivity, $n_{\rm o}$ and $n_{\rm e}$ are the refractive indexes of ordinary and extraordinary light respectively, d is the thickness of waveplate and λ is the wavelength. Mueller matrix error $\Delta M_{\rm wp}$ of the waveplate can be calculated from $\Delta M_{\rm wp} = |M^i_{\rm wp} - M_{\rm QWP}|$. Similarly, it is easy to obtain that none of $\Delta M_{\rm wp}(1,2)$, $\Delta M_{\rm wp}(2,1)$, $\Delta M_{\rm wp}(3,3)$, $\Delta M_{\rm wp}(3,4)$, $\Delta M_{\rm wp}(4,3)$, and $\Delta M_{\rm wp}(4,4)$ are zero, and $\Delta M_{\rm wp}(1,2) = \Delta M_{\rm wp}(2,1)$, $\Delta M_{\rm wp}(3,3) = \Delta M_{\rm wp}(4,4)$, and $\Delta M_{\rm wp}(3,4) = \Delta M_{\rm wp}(4,3)$. Figure 4 shows the calculation results of three Mueller matrix elements $M_{\rm wp}(1,2)$, $M_{\rm wp}(3,3)$, and $M_{\rm wp}(3,4)$ of a zero-order quarter waveplate with reflectivity R theoretically for the case of a quarts material with refractive index values $n_{\rm o} = 1.54697631$ and $n_{\rm e} = 1.556177127$, and $d = 0.0144661$ mm at $\lambda = 532.4$ nm. The reflectivity R must be less than 0.0004 if we want to ensure the crosstalk among Stokes I Q U, and V within 10^{-3}.

$$M^i_{\rm wp} = \begin{bmatrix} 1 & \dfrac{T_{\rm o}-T_{\rm e}}{T_{\rm o}+T_{\rm e}} & 0 & 0 \\ \dfrac{T_{\rm o}-T_{\rm e}}{T_{\rm o}+T_{\rm e}} & 1 & 0 & 0 \\ 0 & 0 & \dfrac{2\sqrt{T_{\rm o}T_{\rm e}}}{T_{\rm o}+T_{\rm e}}\cos\delta & \dfrac{2\sqrt{T_{\rm o}T_{\rm e}}}{T_{\rm o}+T_{\rm e}}\sin\delta \\ 0 & 0 & -\dfrac{2\sqrt{T_{\rm o}T_{\rm e}}}{T_{\rm o}+T_{\rm e}}\sin\delta & \dfrac{2\sqrt{T_{\rm o}T_{\rm e}}}{T_{\rm o}+T_{\rm e}}\cos\delta \end{bmatrix}, \tag{8}$$

$$\begin{aligned} T_{\rm o} &= \frac{(1-R)^2}{1+R^2-2R\cos(2\delta_{\rm o})}, \\ T_{\rm e} &= \frac{(1-R)^2}{1+R^2-2R\cos(2\delta_{\rm e})}, \\ \delta_{\rm o} &= \frac{2\pi n_{\rm o} d}{\lambda}, \\ \delta_{\rm e} &= \frac{2\pi n_{\rm o} d}{\lambda}. \end{aligned} \tag{9}$$

3.2.3. Misalignment of fast axis

Misalignment of fast axis, for the zero order or achromatic waveplate, is another error source, which must be taken into account. The true zero waveplate made of a single piece of material is too thin to be fabricated, usually two thicker pieces may be used, with the fast axis of one piece aligned parallelly to the slow axis of the other to cancel out retardations

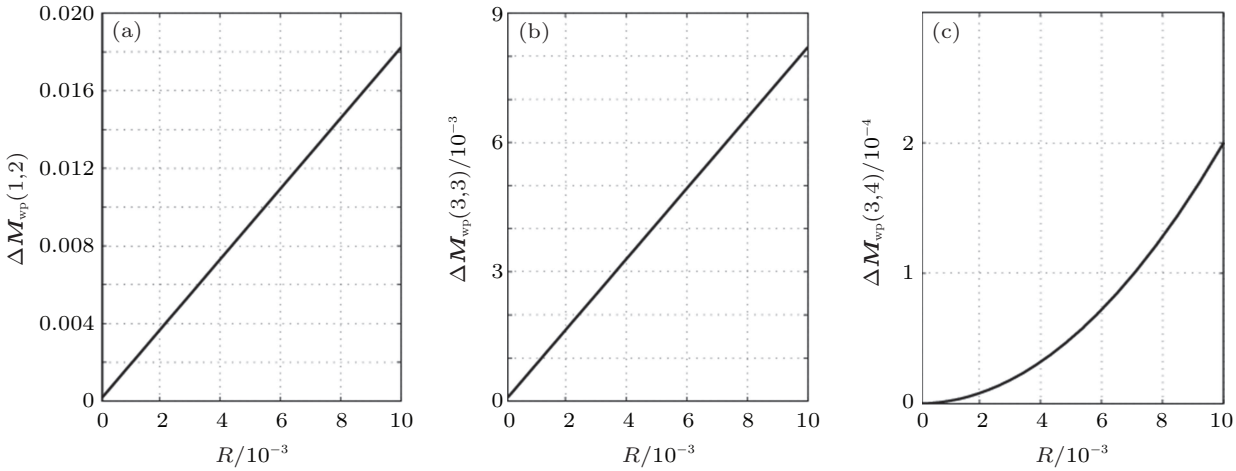


Fig. 4. Dependence of Mueller matrix element errors (a) $\Delta M_{wp}(1,2)$, (b) $\Delta M_{wp}(2,1)\Delta M_{wp}(3,3)$, and (c) $\Delta M_{wp}(3,4)$ of a quarter waveplate on reflectivity.

all but the desired retardation: the two thicker pieces are called zero-order waveplates. Besides, achromatic waveplates which have almost the same retardations over a given wavelength range can be made from two or more different materials. The combined waveplates are widely used in optical instrumentation and the residual errors associated with these devices can be very important in high-resolution spectro-polarimetry measurements. The misalignment of fast axis in a double or more crystal waveplates is one of the main sources of error and leads to elliptical eigenpolarization modes in the retarder and the oscillation of its orientation according to the wavelength.[18]

$$M_{wp}^{m} = R(\Delta\theta)M_{\perp}R(-\Delta\theta)M_{\parallel}, \tag{10}$$

$$R(\Delta\theta) = \begin{bmatrix} 1 & 0 & 0 & 0 \\ 0 & \cos\Delta\theta & -\sin\Delta\theta & 0 \\ 0 & \sin\Delta\theta & \cos\Delta\theta & 0 \\ 0 & 0 & 0 & 1 \end{bmatrix}, \tag{11}$$

$$R(-\Delta\theta) = \begin{bmatrix} 1 & 0 & 0 & 0 \\ 0 & \cos\Delta\theta & \sin\Delta\theta & 0 \\ 0 & -\sin\Delta\theta & \cos\Delta\theta & 0 \\ 0 & 0 & 0 & 1 \end{bmatrix}, \tag{12}$$

$$M_{\perp} = \begin{bmatrix} 1 & 0 & 0 & 0 \\ 0 & 1 & 0 & 0 \\ 0 & 0 & \cos\delta_{\perp} & -\sin\delta_{\perp} \\ 0 & 0 & \sin\delta_{\perp} & \cos\delta_{\perp} \end{bmatrix}, \tag{13}$$

$$M_{\parallel} = \begin{bmatrix} 1 & 0 & 0 & 0 \\ 0 & 1 & 0 & 0 \\ 0 & 0 & \cos\delta_{\parallel} & \sin\delta_{\parallel} \\ 0 & 0 & -\sin\delta_{\parallel} & \cos\delta_{\parallel} \end{bmatrix}, \tag{14}$$

$$\delta_{\parallel} = \frac{2\pi\Delta n d_{\parallel}}{\lambda}, \quad \delta_{\perp} = \frac{2\pi\Delta n d_{\perp}}{\lambda}. \tag{15}$$

The waveplate's eigen Mueller matrix with misalignment of fast axis can be described by Eqs. (10)–(15), where $\Delta\theta$ is the misalignment angle of fast axis, $\Delta n = n_o - n_e$ is the birefringence index, $d_{\parallel}$ and $d_{\perp}$ are the thickness of both plates. Mueller matrix error of the waveplate can be calculated from $\Delta M_{wp} = |M_{wp}^{m} - M_{QWP}|$ where only the first row and the first column are zero. Figure 5 shows the calculation results of nine Mueller matrix nonzero elements of a zero-order quarter waveplate with misalignment of fast axis, with setting data $n_o = 1.54697631$, $n_e = 1.556177127$, $d_{\parallel} = 1.0144661$ mm, and $d_{\perp} = 1$ mm at $\lambda = 532.4$ nm. The misalignment angle of fast axis must be less than 0.03° if we want to control the crosstalk to be within 10^{-3}.

3.2.4. Field of view effect

The field of view (FOV) effect is unavoidable for any waveplate described above, and it mainly leads to retardation variation with FOV. Generally, the retardation of a uniaxial crystal can be described by Eqs. (16) and (17), where ϕ is the azimuth angle. Figure 6 gives the FOV effect of zero-order quarter waveplate made of quartz crystal with FOV. It is known from Eq. (6) that FOV effect induces the FOV-dependent distribution of $\Delta M_{wp}(3,3)$, $\Delta M_{wp}(3,4)$, $\Delta M_{wp}(4,3)$, and $\Delta M_{wp}(4,4)$ as shown in Fig. 7. In the collimation optical path, each spatial point of quarter waveplate undergoes the same incident angle and thickness, and the retardation value only depends on FOV, which is the same as the scenario in Fig. 7. The FOV must be limited within 0.5° if the crosstalk is required to be within 10^{-3}. In a convergent optical path, i.e., another way each spatial point undergoes different incident angles and thickness, the total retardation value is a superposition of different incident angles. After averaging $M_{wp}(3,3)$ and $M_{wp}(3,4)$ in Fig. 7 over all the FOVs, we obtain the mean values of $\Delta M_{wp}(3,3)$ and $\Delta M_{wp}(3,4)$ to be 1.24×10^{-4} and 4×10^{-4}, respectively, far less than 10^{-3}. Therefore, the crosstalk induced by convergent optical path is very small and can be ignored.

$$\delta = \frac{2\pi d}{\lambda}\left(\frac{A_1}{n_o} - A_2\right), \tag{16}$$

$$A_1 = \sqrt{n_e^2 n_o^2 - (n_e^2\cos^2\phi + n_o^2\sin^2\phi)\sin^2(FOV)},$$

$$A_2 = \sqrt{n_o^2 - \sin^2(FOV)}. \tag{17}$$

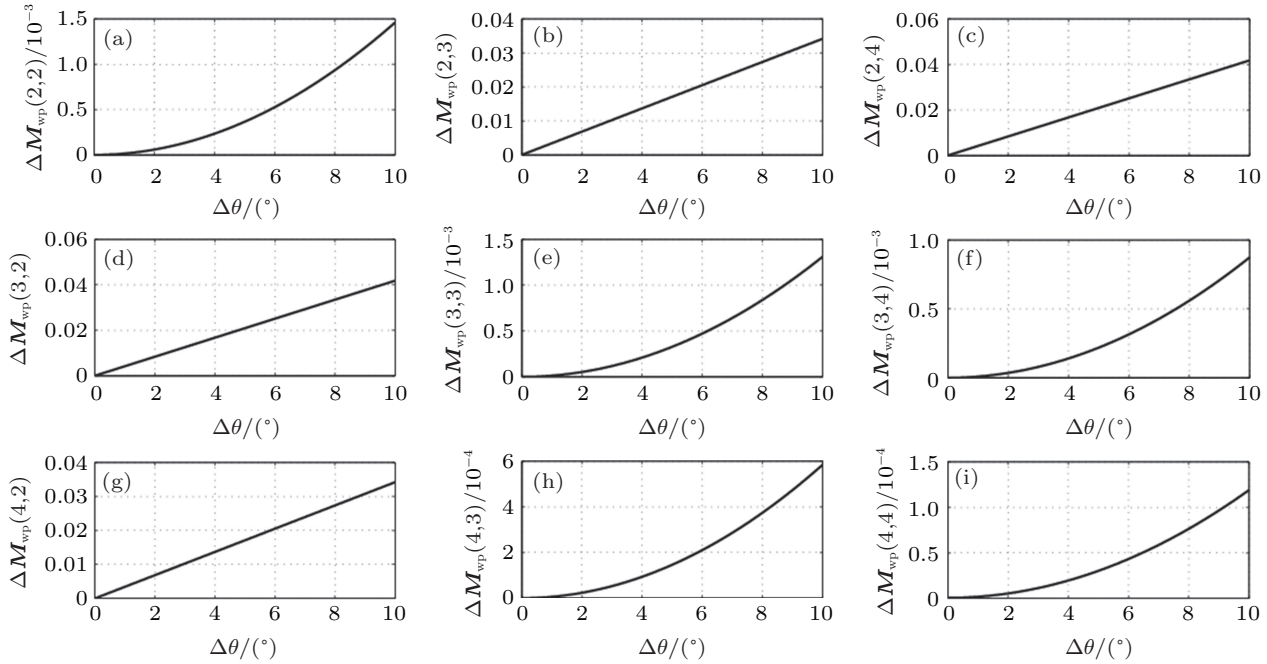


Fig. 5. Dependence of Mueller matrix element errors (a) $\Delta \boldsymbol{M}_{\rm wp}(2,2)$, (b) $\Delta \boldsymbol{M}_{\rm wp}(2,3)$, (c) $\Delta \boldsymbol{M}_{\rm wp}(2,4)$, (d) $\Delta \boldsymbol{M}_{\rm wp}(3,2)$, (e) $\Delta \boldsymbol{M}_{\rm wp}(3,3)$, (f) $\Delta \boldsymbol{M}_{\rm wp}(3,4)$, (g) $\Delta \boldsymbol{M}_{\rm wp}(4,2)$, (h) $\Delta \boldsymbol{M}_{\rm wp}(4,3)$, and (i) $\Delta \boldsymbol{M}_{\rm wp}(4,4)$ of a quarter waveplate on misalignment angle of fast axis.

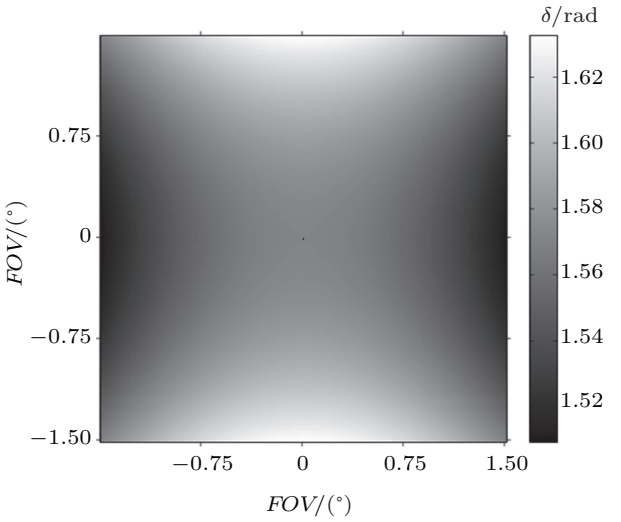


Fig. 6. FOV effect of zero-order quarter waveplate made of quartz crystal with FOV.

3.3. Tolerance analysis

Table 1 lists the tolerances of all the error sources with requirement for crosstalk less than 10^{-3} according to Subsection 3.2. The tolerances, induced by extinction ratio and FOV effect in a convergent path, are loose. Contrarily, the other ones are very strict. More specifically, it is known from tolerance analysis that the large measurement errors are mainly from four error sources: retardation error, interference, misalignment of fast axis and FOV effect in collimated path. The four error sources are all impossible for PCU in manufacture to meet the calibration requirement of telescope. The polarimetric accuracy of the calibration will depend strongly on these imperfect properties of the PCU. Therefore, An improved polarization calibration method is desired for PCU to calibrate and calculate these errors, hence eliminating the effects from these errors.

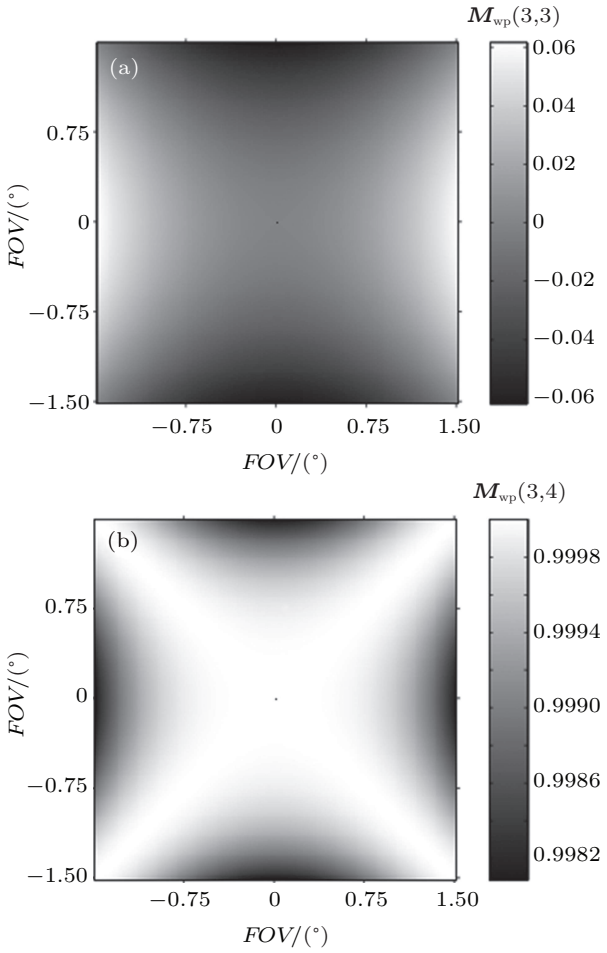


Fig. 7. The Distributions of (a) $\boldsymbol{M}_{\rm wp}(3,3)$ and (b) $\boldsymbol{M}_{\rm wp}(3,4)$ of zero-order quarter waveplate with variation of FOV.

Table 1. Tolerances of error sources.

Error sources	Parameters	Tolerance
Extinction ratio	ER	2000:1
Retardation error	$\Delta\delta$	0.001 rad
Interference	R	0.0004
Misalignment of fast axis	$\Delta\theta$	0.03°
Field of view effect (collimated)	FOV	0.5°
Field of view effect (convergent)	FOV	ignored

It is noted that we have not considered the beam deviation of light beam induced by rotating waveplate and polarizer, in error analysis of PCU. Because we have proposed a new method in another paper to reduce the first order beam deviation,[19] the error can be ignored.

4. Optimal design of polarization calibration method

4.1. Optimal polarization calibration method

In general, retardation error and FOV effect in collimated path belong to the same type of error, each of which leads to retardation value δ of quarter waveplate being not exactly 90°; Interference mainly affects dichroism and can be described by a parameter "dichroism angle Ψ" (Ψ will be 45° for waveplate without dichroism); The misalignment of fast axis changes a waveplate from linear retarder into elliptical retarder and can also be described by another parameter "ellipticity angle e" (e will be zero for a linear retarder). In optimization, these errors are taken as unknown parameters during the whole calibration procedure, and they will be calculated with the instrumental polarization of telescope simultaneously to remove the effects of these non-ideal properties.

The incident light beam to PCU is conventionally described through the Stokes vector $\boldsymbol{S}_{\rm in} = [I\ Q\ U\ V]^{\rm T}$. Then, the polarized light $\boldsymbol{S}_{\rm c}^{\rm in}$ behind PCU in front of Azi–Alt optics and polarimeter can be completely described by the following function:

$$\begin{aligned}\boldsymbol{S}_{\rm c}^{\rm in} &= \boldsymbol{R}(\theta_{\rm wp}+\theta_0)\boldsymbol{M}_{\rm wp}(\delta,\Psi,e)\boldsymbol{R}(-\theta_{\rm wp}-\theta_0)\\ &\quad\times\boldsymbol{R}(\theta_{\rm p})\boldsymbol{M}_{\rm p}\boldsymbol{R}(-\theta_{\rm p})\boldsymbol{S}_{\rm in}, \end{aligned}\tag{18}$$

$$\boldsymbol{R}(\theta) = \begin{bmatrix} 1 & 0 & 0 & 0\\ 0 & \cos(2\theta) & \sin(2\theta) & 0\\ 0 & -\sin(2\theta) & \cos(2\theta) & 0\\ 0 & 0 & 0 & 1\end{bmatrix},\quad \theta=\theta_{\rm wp},\theta_{\rm p},\tag{19}$$

$$\begin{aligned} a &= \sin(\delta/2)\sin(2e),\\ b &= \cos(\delta/2),\\ c &= \sin(\delta/2)\cos(2e),\\ A &= a^2+b^2+c^2=1,\\ B &= b^2+c^2-a^2,\\ C &= b^2-c^2-a^2,\\ D &= b^2+a^2-c^2, \end{aligned}\tag{20}$$

$$\boldsymbol{M}_{\rm wp} = \begin{bmatrix} 1 & -\cos(2\Psi) & 0 & 0\\ -\cos(2\Psi) & B & 2ab & -2ac\\ 0 & -2ab & C\sin(2\psi) & -2bc\sin(2\psi)\\ 0 & -2ac & 2bc\sin(2\psi) & D\sin(2\psi)\end{bmatrix},\tag{21}$$

$$\boldsymbol{M}_{\rm p} = \begin{bmatrix} 1 & 1 & 0 & 0\\ 1 & 1 & 0 & 0\\ 0 & 0 & 0 & 0\\ 0 & 0 & 0 & 0\end{bmatrix},\tag{22}$$

where $\boldsymbol{R}$ is the rotation matrix; $\boldsymbol{M}_{\rm p}$ and $\boldsymbol{M}_{\rm wp}$ are the Mueller matrices of polarizer and waveplated respectively; adjusting polarizer's transmitted axis to $+Q$ direction; $\theta_{\rm p}$ is the rotation angle of polarizer's transmitted axis relative to $+Q$ direction; θ_0 is the origin angle of waveplate's fast axis relative to $+Q$ direction; $\theta_{\rm wp}$ is the rotation angle of waveplate's fast axis relative to its original direction; δ, Ψ, and e are retardation, dichroism angle and ellipticity angle of waveplate respectively. We suppose that the polarizer is perfect, which is reasonable because the extinction ratio of the polarizer employed is larger than 2000:1. Thus, the general equation between the calibrated Stokes vector $\boldsymbol{S}_{\rm c}^{\rm in}$ and measured output $\boldsymbol{S}_{\rm c}^{\rm out}$ during the calibration is given by,

$$\boldsymbol{S}_{\rm c}^{\rm out} = \boldsymbol{X}'\boldsymbol{S}_{\rm c}^{\rm in},\tag{23}$$

where $\boldsymbol{X}'$ is derived from the measurements after arranging the calibrated Stokes vectors into an optimal 4 by 6 matrices by rotating polarizer and waveplate of PCU at the following angles respectively,

$$\begin{bmatrix}\theta_{\rm wp}\ \theta_{\rm p}\end{bmatrix} = \begin{bmatrix} 0^\circ & 0^\circ\\ 45^\circ & 45^\circ\\ 90^\circ & 90^\circ\\ 135^\circ & 90^\circ\\ 135^\circ & 135^\circ\\ 135^\circ & 180^\circ\end{bmatrix}.\tag{24}$$

In Eqs. (18)–(22), there are another 7 parameters in addition to the 16 elements of $\boldsymbol{X}'$:

– The incident Stokes parameters Q, U, and V;

– An offset angle, θ_0, between PCU polarizer and retarder to account for misalignment;

– Retardation δ, dichroism Ψ and ellipticity e of waveplate, including all the four main errors of PCU.

The 23 free parameters are all computed by minimizing the χ^2 value,

$$\chi^2 = \sum_{i=0,\ldots,3} (\tilde{\boldsymbol{I}}_{\rm c}^{\rm out} - \boldsymbol{I}_{\rm c}^{\rm out})_i^2 \tag{25}$$

where $\tilde{\boldsymbol{I}}_{\rm c}^{\rm out}$ and $\boldsymbol{I}_{\rm c}^{\rm out}$ are the measured values and the theoretical values of the polarization measurement and calibration system.

4.2. Error control and simulation

Intensity instability of the incident beam is the main error source. On the one hand, the sun is the only light source in calibration process, and it is easily disturbed by seeing, thus leading to intensity instability; on the other hand, the instrumental polarization of Alt–Azimuth optics changes over time strongly, the faster the better for calibration, but it is difficult in this case to improve signal-to-noise ratio of incident intensity by operating long time exposure and integration. A numerical simulation will efficiently demonstrate the relevance of the calibration error tointensity instability.

Numerical simulation process is as follows:

(i) simulate a group of original values of the incident Stokes parameters Q, U, V, the parameters of PCU δ, Ψ, e, and the polarized response matrix $\boldsymbol{X}'$ of the whole telescope combined with Alt–Azimuth mounted optics and Stokes polarimeter according to Section 2, Subsection 4.1, and NVST's polarization model;[11]

(ii) simulate a group of observation data $\tilde{\boldsymbol{I}}_{\rm c}^{\rm out}$ based on the original values above and Subsection 4.1;

(iii) add different intensity instabilities from 10^{-1} to 10^{-4} to each element of $\tilde{\boldsymbol{I}}_{\rm c}^{\rm out}$ and simulate the real measurement state;

(iv) calculate $\tilde{\boldsymbol{X}}'$ through the optimal polarization calibration method;

(v) calculate the calibration error from intensity instability by $\Delta\boldsymbol{X}' = |\boldsymbol{X}' - \tilde{\boldsymbol{X}}'|$;

(vi) repeat the above steps (iii)–(v) 100 times, the root mean square (RMS) of $\Delta\boldsymbol{X}'$ will be used to evaluate the relevance of the calibration error to intensity instability.

The time-dependent polarized response matrix $\boldsymbol{X}'$ in one day are shown in Fig. 8, from which we can evaluate relationship between the calibration error and intensity instability in different time, which is very important for Alt–Azimuth mounted telescope because its instrumental polarization varies greatly during a day. Besides, set $Q = 0.01$, $U = -0.02$, $V = 0$, $\delta = 96°$, $\Psi = 48°$ and $e = 2°$. Figure 9 displays the simulated results, where the longitudinal coordinate is RMS of calibration error of $\boldsymbol{X}'$ obtained using the optimal calibration method, different colors represent different intensity instabilities from 10^{-1} to 10^{-4}, the unit of longitudinal coordinate is log10 (logarithm). It is shown by comparing Eq. (3) and Fig. 9 that the intensity instability must be less than 10^{-3} if controlling calibration accuracy goes up to 10^{-4}, also the trends almost do not change with time during a day. Noted that the cross-talk from I to QUV is a little larger than 10^{-4} in instability 10^{-3}, however, the crosstalk can be removed by observing the quiet sun without using the optimal calibration method.

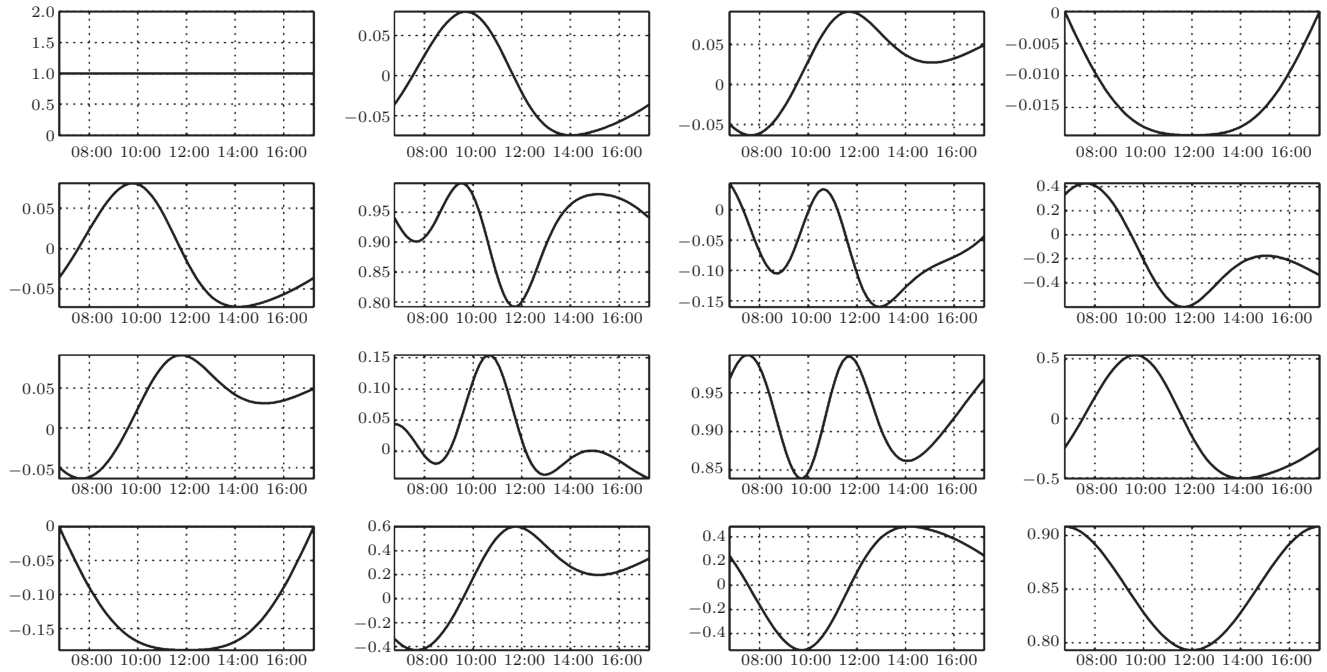


Fig. 8. Simulated polarized response matrix $\boldsymbol{X}'$ of the whole telescope combined with Alt–Azimuth mounted optics and Stokes polarimeter based on NVST's polarization model. x axis is time, y axis is variations of each element in $\boldsymbol{X}'$ with time during a day.

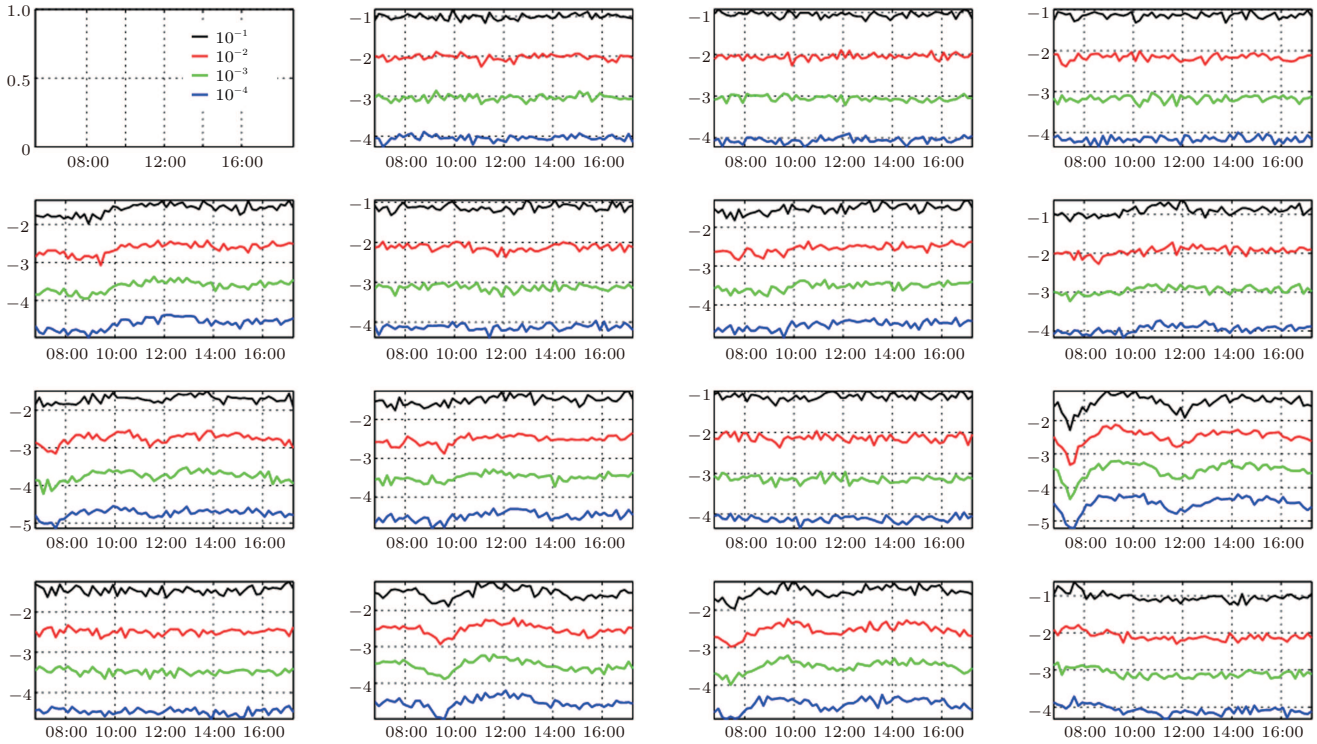


Fig. 9. (color online) Relations of calibration error and intensity instability. x axis is time, y axis is variations of each element in RMS of $\Delta \boldsymbol{X}'$ with time during a day.

5. Conclusions

The polarimetric accuracy of the calibration depends strongly on property of the PCU. We analyze the main measurement errors and tolerance errors induced by an imperfect PCU, and it is found that the errors from extinction ratio and field of view effect in convergent path, are small and can be ignored in calibration. But, the main error sources affecting calibration accuracy are retardation error, interference, misalignment of fast axis and FOV effect in collimated path.

We optimize the calibration method for PCU. Classical method does not take into account the non-ideal properties of PCU, such as incident linear polarization, dichroism and ellipticity of retarder, etc. In our optimization, these errors are taken as unknown parameters during the whole calibration procedure, and they are calculated with the instrumental polarization of telescope simultaneously to remove effects of these non-ideal properties.

Intensity instability of the incident beam is the main error source. A numerical simulation is given to evaluate the relevance of the calibration error to intensity instability. Results show that the intensity instability must be less than 10^{-3} if controlling calibration accuracy goes up to 10^{-4}.

References

[1] Hale G E 1908 *ApJ* **28** 315
[2] Unno W 1956 *PASJ* **8** 108
[3] Li K W, Wang Z B, Li S W, *et al.* 2015 *Acta Phys. Sin.* **64** 140702 (in Chinese)
[4] Zhang Z G, Deng F L, Zhang Q C, *et al.* 2014 *Acta Phys. Sin.* **63** 184204 (in Chinese)
[5] Keil S, Rimmele T, Keller C, *et al.* 2003 *Astron. Nachr.* **324** 303
[6] Bettonvil F C M, Collados M, Feller A, *et al.* 2010 *Proc. SPIE Ground-based and Airborne Instrumentation for Astronomy III*, July 20, 2010, San Diego, California, USA, p. 77356
[7] Liu Z h, Deng Y Y, Ji H S h, *et al.* 2012 *Sci. Sin.-Phys. Mech. Astron.* **42** 1282
[8] Elmore D 2010 *Astron. Nachr.* **331** 655
[9] Hector S N 2005 *J. Opt. Soc. Am. A* **22** 539
[10] Hector S N 2005 *J. Opt. Soc. Am. A* **22** 907
[11] Yuan S 2014 *Solar Polarization 7*, September 9–13, 2013, Kunming, China, p. 297
[12] Goode P R, Coulter R, Gorceix N, *et al.* 2010 *Astron. Nachr.* **331** 620
[13] Beck C, Schmidt W, Kentischer T, *et al.* 2005 *A & A* **437** 1159
[14] Skumanich A, Lites B W, Pillet V M, *et al.* 1997 *ApJ* **110** 357
[15] Ichimoto K, Shinoda K, Yamamoto T, *et al.* 2006 *Publ. Natl. Astron. Obs. Japan* **8** 11
[16] Ichimoto K, Lites B, Elmore D, *et al.* 2008 *Solar Phys.* **249** 223
[17] Clarke D 2004 *J. Opt. A: Pure Appl. Opt.* **6** 1036
[18] Boulbry B, Jeune B, *et al.* 2001 *Opt. Exp.* **9** 225
[19] Hou J F, Wang D G, Deng Y Y, *et al.* 2015 *Acta Phys. Sin.* **64** 060701 (in Chinese)